Title: Natural evolution of SARS-CoV-2 variants in K18-ACE2 mice gives rise to more virulent virus and variant alleles associated with treatment resistance.

Authors: Julian Daniel Sunday Willett[1,2,3], Annie Gravel[4], Isabelle Dubuc[4], Leslie Gudimard[4], Paul Fortin[4,5,6], Ju-Ling Liu[2,8], Jose Hector Galvez[7], Melissa Zwaig[2,8], Anne-Marie Roy[2,8], Sally Lee[2,8], Shu-Huang Chen[2,8],Jiannis Ragoussis[2,8]*, Louis Flamand[4,9]*

Affiliations:

1. Quantitative Life Sciences Ph.D. Program, McGill University, Montreal, QC, Canada
2. McGill University Genome Centre, Montreal, QC, Canada
3. Lady Davis Institute, Jewish General Hospital, Montreal, QC, Canada
4. Axe maladies infectieuses et immunitaires, Centre de Recherche du Centre Hospitalier Universitaire de Québec- Université Laval, Canada
5. Centre de Recherche ARThrite-Arthrite, Recherche et Traitements, Université Laval, Québec, QC, Canada.
6. Division of Rheumatology, Department of Medicine, CHU de Québec-Université Laval, Québec, QC, Canada
7. Canadian Centre for Computational Genomics, McGill University, Montreal, QC, Canada
8. Department of Human Genetics, McGill University, Montreal, QC, Canada
9. Département de microbiologie-infectiologie et d'immunologie, Université Laval, QC, Canada.

*Co-corresponding authors

Abstract:

Background: The continuing COVID-19 pandemic is partially due to viral evolution decreasing vaccine and treatment efficacies. Predicting viral evolution is difficult. Others have found that serial infections of the original SARS-CoV-2 isolate in non transgenic mice is accompanied with selection of alleles (such as Spike 417N, 493H and 501Y) conferring adaptation and greater binding affinity for the murine Ace2 receptor, enhanced infectivity, and lethal phenotype in mice. We designed a study to investigate long-term viral evolution's impact in K18-ACE2 mice, mice expressing the human ACE2 receptor, with virus closer related to the Omicron sub-lineage.

Methods: We serially infected SARS-CoV-2-naïve mice with either the B.1.351 (Beta) or the B.1.617.2 (Delta) variant across twenty passages without experimental selective pressures. We sequenced virus across passages, annotating variant alleles changing in frequency, tracking alleles suspected of decreasing vaccine/treatment efficacy. We evaluated virulence in animals infected with virus isolated at study completion and determined antibody neutralization sensitivity using sera from vaccinated individuals.

Results and Conclusions: We observed variant alleles with documented roles in vaccine-elicited immunity evasion. This included the Omicron-associated mutation spike S371F that arose *de-novo* during our study. Passage 20 (P20) viruses were more virulent that their P0 counterpart with P20 Delta lineage being significantly more resistant to antibody neutralization. These developments occurred within two months of the study starting, suggesting that our model can rapidly emulate pandemic progression in mammals. While our model lacked experimental selective pressures, such as pre-existing SARS-CoV-2 immunity, these conditions could readily be adapted. Such modeling could enable development of more evolution-resistant treatments.

Keywords: SARS-CoV-2, COVID-19, pandemic modelling, treatment resistance, viral evolution.

Background:

Part of the difficulty in responding to COVID-19 has been predicting viral evolution and its impact on clinically relevant traits, such as infectivity, treatment resistance, and disease severity (1). The basic biology of the severe acute respiratory syndrome Coronavirus 2 (SARS-CoV-2), the virus that causes COVID-19, is well understood. However, our knowledge of SARS-CoV-2 evolution is limited. Many RNA viruses, such as SARS-CoV-2, exist as quasi-species meaning that within a given viral population, a multitude of alleles (major and minor) are constantly present. These alleles give plasticity to the viral population allowing for rapid adaptation/selection to a variety of circumstances (2). Viral evolution is also complex and affected by several factors, including host genetic background (3), host immune status (4), the organs targeted by the virus (5), and a population's collective immunity (6). As a result, it has been difficult to predict the emergence of new variants with altered virulence.

Several variants of concern (VOC) have emerged, each with mutations providing dissemination advantages (1). For example, the SARS-CoV-2 alpha variant (B.1.1.7) gained a growth advantage and rapidly spread globally due to the spike protein N501Y mutation that enhances affinity for the cellular entry receptor, angiotensin-converting enzyme 2 (ACE2) (7). Other VOC, such as the Delta (B.1.617.2) variant, gained advantages with additional substitutions in spike, including L452R (8), T478K (9), and P681R (10) that affect viral transmissibility and antibody neutralization for naturally or artificially vaccinated individuals (11). To better predict changes in SARS-CoV-2 and reduce the impact of a future pandemic, time effective models must be defined for studying viral changes over successive generations.

71 In 2020, Gu *et al.* studied short-term viral evolution by infecting aged mice with the SARS-CoV-2
72 reference strain (IME-BJ05) and collecting lung tissue at set timepoints following infection, using
73 this isolate to infect successive generations of mice (12). While wild-type mice are thought less
74 susceptible to the virus as mouse Ace2 is not used by SARS-CoV-2 as its receptor, Gu *et al.*
75 demonstrated that serial passaging of lung homogenate across mice produced a mouse-
76 adapted strain (MASCp6) that causes pulmonary symptoms, matching adaptations observed by
77 others who previously applied the technique to influenza (12, 13). After six passages, they found
78 several clinically relevant genetic changes, including de-novo appearance of A23063T that
79 changes spike to N501Y (12). This mutation is associated with enhanced viral infection and
80 transmission (7). Subsequently, the group passaged the MASCp6 isolate an additional 30 times
81 and characterized the MASCp36 isolate (14). MASCp36 contained several mutations (i.e.
82 K417N, Q493H and N501Y mutations) in spike conferring greater ACE2 receptor binding
83 affinity, increased infectivity and greater virulence (14). Others replicated this study using the
84 same viral variant, observing similar development of clinically relevant variant alleles (15).

85 Since these studies, new lineages arisen, with the present being Omicron, negatively impacting
86 treatment efficacy (1). Others have studied viral dynamics using recent lineages in serial
87 passages in cells, observing similar development of directional selection and clinically
88 concerning mutations (16, 17). Given the pandemic's prolonged nature, understanding
89 longitudinal viral changes in a mammalian host is pressing. We adapted Gu *et al.*'s approach to
90 evaluate how viral lineages more closely related to the present lineages, B.1.351 (Beta) and
91 B.1.617.2 (Delta), changed over twenty passages (12) in transgenic mice with human ACE2
92 receptors. Given clinically relevant mutations arising in Gu *et al.*'s studies (12, 14), we sought to
93 determine if impactful variant alleles would develop in more recent viral variants. We report on
94 the *de novo* appearance and persistence of variant alleles associated with treatment resistance
95 with serially passaged virus demonstrating increased viral virulence and antibody resistance.

96 **Methods:**

97 ***Viruses.*** SARS-CoV-2 Wuhan-like strain (LSPQ, B1 lineage) was obtained from the Laboratoire
98 de Santé Publique du Québec ([LSPQ] Sainte-Anne-de-Bellevue, QC, Canada). SARS-CoV-2
99 Beta strain was obtained from BEI resources and SARS-CoV-2 Delta strain from the BC
100 Centers for Disease Control. SARS-CoV-2 strains were propagated on Vero cells (American
101 Type Culture Collection, Manassas, Virginia, USA).

102 ***Determination of the viral titer*.** Vero cells were plated in a 96-well plate ($2x10^4$/well) and
103 infected with 200µl of serial dilution of the viral preparation or lung homogenate in the M199
104 media supplemented with 10mM HEPES pH 7.2, 1mM of sodium pyruvate, 2.5g/L of glucose,
105 5µg/mL *Plasmocin*® and 2% FBS. Three days post-infection plates were analyzed using a
106 EVOS M5000 microscope (ThermoFisher Scientific, Waltham, MA, USA) and the viral titer was
107 determined using the Karber method (18).

108 ***Mouse models***. B6.Cg-Tg(K18-hACE2)2Prlmn/J (stock#3034860) and B6 mice were
109 purchased from the Jackson Laboratories (Bar Harbor, ME). One K18-ACE2 mouse was
110 intranasally infected with either B.1.351 (Beta) or B.1.617.2 (Delta) SARS-CoV-2 lineages.
111 Following 3-4 days, the animals were sacrificed and lung homogenate collected. The
112 homogenate was used to intranasally infect sequential animals, defined as passage. This was
113 repeated for 10 passages. After passage 10 (P10), virus in lung homogenate was sequenced.
114 K18-ACE2 mice were then intranasally infected with Beta P10 or Delta P10 with viruses
115 passaged in three mice at a time for an additional 10 times (total of 20 passages) with virus in
116 lung homogenate sequenced following passages 13, 17, and 20 (**Figure 1**). Viral stocks were
117 then made from lung homogenates of Beta and Delta P20 viruses. K18-ACE2 mice were
118 infected intranasally with 500 $TCID_{50}$ of P0 or P20 viruses. Lung viral loads were determined on
119 day 3 post-infection with weight loss and survival monitored daily for up to 9 days.

120 ***Infectivity of P0 and P20 viruses to non-transgenic mice***. C57BL6 mice were infected
121 intranasally with 3000 $TCID_{50}$ of P0 and P20 Beta and Delta viruses. Three days later, mice
122 were euthanized, and lungs collected for viral load (titer) determination.

123 ***RNA extraction***: Up to 30 mg of lung tissue were used for RNA extraction using the Bead Mill
124 Tissue RNA Purification Kit and the Bead Mill Homogenizer, following manufacturer's
125 instructions.

126 ***Viral sequencing***. RNA extracts were processed for reverse transcription (step a) and targeted
127 SARS-CoV-2 amplification using the ARTIC V3 or V4.1 primer scheme (https://github.com/artic-
128 network/primer-schemes/tree/master/nCoV-2019) (step b). Samples were purified (step b) and
129 Nextera DNA Flex library preparation (step c) was performed for Illumina PE150 paired-end
130 amplicon sequencing on a NovaSeq or MiSeq instrument at the McGill Genome Centre using
131 best practices. Each sample was sequenced twice on different days to obtain a target of
132 minimum 10 million reads per sample. The detailed protocols can be accessed with the
133 following links.

134 Step a: dx.doi.org/10.17504/protocols.io.bjgekjte.

135 Step b: dx.doi.org/10.17504/protocols.io.ewov18e4ygr2/v2.

136 Step c: dx.doi.org/10.17504/protocols.io.bjgnkjve.

137

138 ***Genome data processing*.** Following sequencing, the reads from each sample were used to
139 call variants using Freebayes v1.3.6 (19) and the results were saved as a VCF file which was
140 used to compare genomic variation across passages. Others have called variants with other
141 tools such as DeepSNV (20) and VarScan (21). DeepSNV was not used as it only investigates
142 SNVs (22), when indels have been found to confer selective advantages (23). Freebayes has

143 been observed to perform slightly superiorly than VarScan when calling variants in wastewater
144 samples (24) and in internal benchmarking (data not shown). The process is described briefly
145 as follows: first, the raw reads from each sample were aligned with BWA MEM v0.7.17 (25) to
146 the reference strain genome sequence (NC_045512.2). The resulting alignments were sorted
147 with duplicate reads flagged. The minimum number of aligned reads for each was logged, and
148 each sample was again aligned and processed, then randomly down sampled to match this
149 minimum number of reads. All variants with a quality of less than 20 or a depth below 10 were
150 removed from the analysis. Any variant alleles that overlapped with ARTIC sequencing primers
151 were also removed. Merged VCF files, representing the combination of reads across two
152 sequencing batches for each sample, were used for the paper's main results.

153 ***Variant annotation***. Every variant allele was inputted into COVID-19 Ensembl variant effect
154 predictor (VEP) (https://covid-19.ensembl.org/index.html) to determine functional consequences
155 and the involved gene and amino acid change (26). Variants whose VAF changed at least once
156 across passages during the study were logged and input to the UCSC Genome Browser
157 (https://genome.ucsc.edu/), checking for annotations of antibody escape, CD8 escape, vaccine
158 targets, drug resistance, or variants of concern (27).

159 ***Antibody neutralization studies***. Sera from twenty-four healthy vaccinated (3x) individuals
160 were analyzed for neutralizing activity against Wuhan-like, and Beta and Delta P0 and P20
161 viruses. Serially diluted sera (in quadruplicate) were incubated with 100 $TCID_{50}$ of virus for 1 h
162 at 37˚C before addition to Vero E6 cells. Three days later, the 96-well plates were observed
163 using an inverted microscope for signs of infection. Neutralization titers were determined and
164 defined as the highest serum dilution preventing infection.

165 ***Ethics***. The study was conducted in accordance with the Declaration of Helsinki, and mouse
166 protocols were approved by the Comité de protection des animaux de l'Université Laval. Sera
167 obtained from humans were procured following ERB approval (ERB #2022-6204).

168 ***Statistics***. All statistical analyses were conducted using R/4.2.1. All statistical comparisons
169 between passages were corrected for multiple testing using a Benjamini-Hochberg p-value
170 adjustment.

171 ***Source code***. All code used in this study, from sample processing to data analysis, are publicly
172 available on Github at the following link:
173 https://github.com/juliandwillett/SARS_CoV_2_Serial_Passaging_Study.

174 ***Data availability***. VCF files used to complete computational analyses are available by
175 reasonable request.

176 ***Funding***. This study was supported by the Canadian Institutes for Health Research (CIHR
177 476575) operating grant to the Coronavirus Variants Rapid Response Network (CoVaRR-Net)
178 to LF and IR and CIHR grant (GA1-117694) to LF.

179

180 **Results**:

181 *Variant allele frequency of alleles across passages*. The minimum number of reads per sample
182 across P13, P17, and P20 was 34,253,784. In Beta lineage, there was a significantly lower
183 variant allele frequency (VAF) in P17 and P20 versus other passages (adjusted p-value < 0.05),
184 with a significant difference in Delta comparing P10 and P20 (**Figure 2a-b**). As there was no
185 significant change in allele depth across the study, these VAF differences could be due to
186 growing allelic diversity. Such significant changes, less consistent with random allelic drift, could
187 align with suggested mechanisms of within-host evolution of the variant allele pool, per Tonkin-
188 Hill *et al*. (20). Sample contamination is less likely as there was no significant difference in VAF
189 or variant allele depth between samples for either viral lineage (**Figure 2c-d**).

190 *Gene involvement and variant allele functional consequence severity did not significantly vary*
191 *across passages*. There was no statistically significant change in the proportion of variant alleles
192 involving a specific gene or severity of variant allele predicted functional consequence across
193 the study (adjusted p-value > 0.05) (**Figure 3**), suggesting that the overall allele population did
194 not significantly change in our model without experimental selective pressures (6).

195 *Development of variant alleles associated with clinically relevant traits*. We observed 82 unique
196 variant alleles across our study. There were 41 whose VAF changed with 32 having clinically-
197 relevant annotations, including interactions with human proteins, mutations that may confer drug
198 resistance, variant alleles associated with the Omicron lineage, mutations associated with
199 antibody escape, and mutations at vaccine targets (**Table 1, Supplemental Table 1**) (27, 28). A
200 notable novel variant included C22674T, or Spike S371F, that arose *de-novo* in two animals in
201 P20 for Beta virus and two animals in P13 for Delta virus (**Figure 4**). The allele is associated
202 with protein interactions, antibody escape, affects a vaccine target, and is an Omicron-specific
203 mutation (**Table 1**) (27, 29). We thus observed an Omicron specific mutation in a study not
204 involving Omicron viral lineages. Several other variants changing in frequency also conferred
205 possible drug resistance and targeted the vaccine site (**Table 1**) (27).

206 Most alleles in the P0 Beta isolate, passaged several times *in vitro* in Vero cells, encoded a
207 Spike protein with a tryptophan (W) at position 682 (C23606T), destroying the furin cleavage
208 site (**Table 1**). We observed a rapid selection of viruses having the reference allele encoding an
209 arginine (R) at position 682 and functional furin site in all animals infected with Beta variant
210 starting in P10 (**Table 1**). This suggests that the furin site provides a growth advantage under *in*
211 *vivo* conditions and supports a previous report indicating the Spike furin site being important for
212 SARS-CoV-2 virulence in K18-ACE2 mice (30).

213 *Later passage virus was linked with greater weight loss, virus producing larger viral loads more*
214 *quickly, and reduced antibody neutralization*. Unlike Gu *et al*.'s study that required adaptation of
215 SARS-CoV-2 to a murine Ace2 receptor for infectivity, our study made use of transgenic mice
216 expressing the human ACE2 receptor (12). We determined whether repeated passaging of
217 SARS-CoV-2 in K18-ACE2 mice affected virulence by infecting animals with P0 and P20 viruses
218 with clinical scores and viral loads determined. On day 3 post-infection, no differences in viral
219 load were noted between Beta P0 and Beta P20 viruses with mice infected with P20 Delta virus
220 having a significant increase (6.3x) in lung viral loads (**Figure 5A**). Both P20 Beta and P20
221 Delta viruses caused more rapid and greater weight loss than P0 viruses (**Figures 5B-C**) with
222 similar survival curves (**data not shown**).

223 We then assessed whether repeated passages in K18-ACE2 mice would result in viruses
224 capable of infecting non transgenic mice. C57BL6 mice were infected intranasally with P0 and
225 P20 viruses and lung infectious viral loads determined 3 days later. Both P0 and P20 Beta
226 viruses successfully replicated in mouse lungs with both viruses producing similar viral loads
227 (**Supplementary Figure 2**). None of the P0 or the P20 Delta viruses generated viral loads in
228 lungs of B6 mice (**Supplementary Figure 2**).

229 Our results indicate that Delta P20 viruses generate a greater viral load that P0. To determine if
230 this was related to growth kinetic differences between P0 and P20 viruses, we performed *in vitro*
231 growth curve analysis. We observed two independently evolved P20 Delta viruses replicating
232 more efficiently after 24 h versus P0, yielding 4-5X more infectious virus after 24h of infection
233 (**Figure 6**). This difference in viral titers was no longer observed after 48 h (**Figure 6**).

234 We next determined the ability of sera from vaccinated subjects to neutralize passaged viruses,
235 comparing it to parental P0 viruses. Consistent with previous reports, sera from vaccinated
236 subjects had varied neutralizing potential depending on the variant, with neutralization titers
237 being greatest against the original Wuhan-like strain and lowest for the Beta isolate (**Figure 7A**)

238 (31, 32). The same sera were analyzed for their ability to neutralize P20 viruses. P20 Beta was
239 neutralized equally (13 out of 24) or more efficiently (8 of 24) that the P0 virus (**Figure 7B**). In
240 contrast, P20 Delta virus was significantly less sensitive to antibody neutralization by vaccinated
241 subject sera than P0 ($p < 0.0002$) where 15 of 24 sera showed decreased neutralizing potential
242 toward the P20 Delta virus relative to P0 (**Figure 7C**).

243

244 **Discussion**:

245 In this study, we serially infected mice with Beta or Delta lineage virus for twenty passages
246 without experimental selective pressures. The evolved viruses developed and maintained
247 variant alleles associated with treatment resistance and later lineages like Omicron (**Figure 4,**
248 **Table 1**), were more virulent (**Figure 5**), grew faster and to higher levels (Delta) (**Figure 6**) and
249 were less sensitive to antibody neutralization (Delta) (**Figure 7**), demonstrating immune escape
250 potential. These developments occurred within roughly two months, illustrating the model's
251 potential in rapidly emulating pandemic progression that could facilitate treatment/vaccine
252 development less sensitive to viral evolution. The model can readily be adapted to mimic viral
253 adaptation in the context of immune or anti-viral selection pressures, affording rapid results in a
254 system often seen in real world conditions.

255 Our model lacked experimental selective pressures, mimicking the evolution of SARS-CoV-2 in
256 a naïve population. Using K18-ACE2 transgenic mice eliminated the selective pressure of
257 adapting virus to the murine Ace2 receptor. The Beta P0 virus harbored the N501Y mutation
258 previously reported to enable adaptation of reference SARS-CoV-2 in non transgenic mice (12).
259 This mutation was maintained throughout passages, suggesting that this virus can infect cells
260 through the murine Ace2 receptor as well (**Figure 4**). Our data supports this, as non transgenic
261 C57BL6 mice were equally susceptible to infection by Beta P0 and P20 viruses. This capacity of

262 Beta to use human and murine receptors might explain, at least in part, the greater virulence of
263 the Beta isolate in ACE2 transgenic mice relative to other viral isolates, such as Wuhan and
264 Delta lacking the N501Y mutation in transgenic mouse studies (33).

265 The Delta P0 virus lacked the N501Y mutation and never acquired it following repeated
266 passages in ACE2 transgenic mice. This highlights that when lacking selective pressure, such
267 as neutralizing antibodies, the appearance of N501Y is not favored (**Figure 4**). Acquisition of
268 N501Y in the human population was first reported almost a year after the initial report of the
269 SARS-CoV-2 epidemic, suggesting that this mutation arose during the development of herd
270 immunity (34).

271 Of the 41 variant alleles that arose *de-novo* or changed in frequency during the study, several
272 are of clinical interest (**Figure 4, Table 1**). A4981G, which arose *de-novo* and persisted in Beta
273 lineage virus in P17 (**Figure 4**), was predicted to possibly confer drug resistance to papain-like
274 protease inhibitors (35), such as ritonavir used clinically in combination with nirmatrelvir that
275 protects patients against severe COVID-19 (36, 37). C22674T, or spike S371F, which arose *de-*
276 *novo* and persisted in two animals in P20 for Beta and P13 for Delta virus (**Figure 4**), represents
277 an Omicron-specific mutation arising in a study that did not use Omicron. This last mutation has
278 been previously reported to facilitate antibody escape (**Table 1**) (29). Considering that the
279 mutation S371F is reported to bear a significant fitness cost (38), this might explain why isolated
280 S371L/F mutations are not viable or have not yet been detected in isolation. We would argue
281 that mutations of residues E484 present in Delta and K417/E484/N501 present in Beta Spike
282 proteins, also found together with the S371F mutation in Omicron BA.2, represent such
283 compensatory mutations. G23593T, or spike Q677H, which disappeared from Beta virus
284 samples after P0, has been determined to enhance treatment resistance and increase viral
285 infectivity (39). The reversion of Spike amino acid 677 to Q after passage in mice could explain
286 the increased neutralization activity for some of the sera against Beta P20 relative to P0 (**Figure**

287 7). Variants that could impair treatment efficacy appeared and disappeared in this study,
288 showcasing the model's potential in evaluating diverse variants.

289 This study has limitations. Here we used the K18-ACE2 transgenic mice but the mechanisms of
290 new viral variants arising in humans could significantly differ. This is relevant as host factors are
291 believed to contribute to viral variant allele diversity (40). Our model lacked experimental
292 selective pressures, while the COVID-19 pandemic has been accompanied by contact
293 limitations and vaccines with the dominant SARS-CoV-2 evolutionary mechanism believed to be
294 natural selection (6). Development or dominance of new variants likely varies with these
295 pressures, necessitating reproducing this model with them. However, a baseline comparison
296 model is required to get the most from these supplemental models, hence the relevance of our
297 model. We studied Beta and Delta lineage virus, which are no longer dominant. Patterns of
298 genetic changes observed in these lineages could vary from Omicron. There was no statistical
299 change in the variant allele population's involvement of specific genes or predicted functional
300 consequence when comparing Beta and Delta lineages across passages, which is reassuring
301 for generalizability. However, virulence significantly increased across the study, despite this lack
302 of population-level changes (**Figure 5**). This could suggest greater value in studying changes in
303 single variant alleles over allele populations, as done in this study, as they are associated with
304 fitness-related traits and can capture evolutionary changes of more subtle mechanisms, such as
305 increasing virus adaptation for cellular infection. Single or combinations of variant allele changes
306 could explain the change in virulence and antibody neutralization observed in this study (**Figure**
307 **4**).

308

309

310

311 **Conclusions**:

312 The model presented rapidly emulated pandemic progression in a naïve population, with virus
313 accumulating variant alleles that could limit therapies for severe disease, becoming more
314 virulent, and ultimately becoming treatment resistant in mice harboring human ACE2 receptor.
315 These results support that serial viral passaging in mice is a useful method to rapidly study viral
316 evolution enabling development of targeted anti-viral therapies.

317

318 **List of abbreviations:**

319 ACE2: angiotensin-converting enzyme 2

320 CIHR: Canadian Institutes for Health Research

321 CoVaRR-Net: Coronavirus Variants Rapid Response Network

322 SARS-CoV-2: severe acute respiratory syndrome Coronavirus 2

323 SNV: single nucleotide variant.

324 $TCID_{50}$: 50% tissue culture infectious dose

325 VAF: variant allele frequency

326 VEP: variant effect predictor

327 VOC: variants of concern

328

329 **Figure Titles and Legends.**

330 **Figure 1**. **Study design**. First, SARS-CoV-2 ACE2-adapted mice were inoculated with either
331 B.1.351 (Beta) or B.1.617.2 (Delta) virus and left for three days for virus to proliferate. They

332 were then sacrificed with the lung homogenate used to infect another mouse. This was repeated
333 for ten passages. Second, P10 virus for each lineage was used to infect three additional mice
334 and the process was repeated for an additional ten passages. Third, P0 and P20 virus for each
335 lineage was used to infect additional mice to compare weight loss and survival between early
336 and late passage virus, and test non-adapted mouse susceptibility to the virus. Antibody
337 neutralization of virus was also compared.

338 **Figure 2. Boxplots of variant allele frequency by (a-b) passage and (c-d) sample.** Each N
339 refers to the number of variant alleles for each MAF and in total against the NC_045512.2
340 reference sequence. Single samples were sequenced for P0 and P10 with three samples from
341 P13, P17, and P20. Box fill in (c-d) signifies sample number. For significance, n.s.: adjusted p-
342 value > 0.05, *: adjusted p-value > 0.01, **: adjusted p-value ≤ 0.01.

343 **Figure 3. Gene involvement and predicted variant allele functional consequence severity**
344 **(VEP) in variant allele population did not significantly change (adjusted p-value > 0.05)**
345 **with passage.**

346 **Figure 4. Variants of clinical relevance arose de novo and grew to dominance**. VAF:
347 variant allele frequency. P refers to passage.

348 **Table 1. Annotations of select variants that changed in frequency across the study.**

349 **Figure 5. Pathogenesis of P0 and P20 viruses in K18-ACE2 mice**. Mice (n = 15/group) were
350 infected with 500 $TCID_{50}$ of P0 or P20 Beta and Delta viruses. (A) On day 3 post-infection, mice
351 (n = 5) were euthanized and lungs collected for infectious viral load determination. Results are
352 expressed as mean ± SD SARS-CoV-2 $TCID_{50}$/mg of lung tissue. (B-C) The weight of each
353 mouse (n = 10/group) was monitored daily throughout the experiment and reported as mean
354 percentage ± SD of weight relative to day 0. **: $p \leq 0.008$ as determined using non-parametric
355 Mann-Whitney test.

356 **Figure 6**. **Growth kinetics of P0 and P20 Delta viruses**. P0 and two independently evolved
357 P20 Delta viruses were used to infect Vero cells at a multiplicity of infection of 0.005. Cell-free
358 supernatants were collected at 24 h and 48 h and used for viral titration. Results are expressed
359 as mean ± SD $TCID_{50}$/mL. *: p=0.02 as determined using an unpaired t-test.

360 **Figure 7.** **Neutralization of P0 and P20 viruses with sera from vaccinated subjects**. (A)
361 Neutralization assay of Wuhan-like, Beta, and Delta viruses using sera from 24 vaccinated
362 subjects. Individual results and mean ± SD neutralization titer against different SARS-CoV-2
363 isolates are presented. ****: p<0.0001 determined using one way-ANOVA. ns: not statistically
364 significant. (B) Pair-wise comparison of the sera used in A in neutralization assay against P0
365 and P20 Beta viruses. (C) Pair-wise comparison of the sera used in A in neutralization assay
366 against P0 and P20 Delta viruses. ***: p>0.002 determined using paired t-test.

367 **Supplemental Table 1**. **Table of variant alleles that changed MAF during the study.**
368 **Available in "Supplemental Tables.csv".**

369 **Supplemental Figure 1**. **Viral load comparison between P0 and P20 virus in K18-ACE2**
370 **mice.**

371 **Supplementary Figure 2**. **Infection of C57BL6 mice with P0 and P20 Beta and Delta**
372 **viruses**. Mice (n = 5/group) were infected intranasally with 3000 $TCID_{50}$ of P0 or three
373 independently evolved Beta P20 or two independently evolved Delta viruses. On the third day
374 post infection, mice were euthanized and lungs collected for infectious viral load determination.
375 Individual results and mean ± SD $TCID_{50}$/mg of lung tissue are presented.

376

377

378

Declarations:

Ethics approval and consent to participate. The study was conducted in accordance with the Declaration of Helsinki, and mouse protocols were approved by the Comité de protection des animaux de l'Université Laval.

Consent for publication: All authors have consented to publication.

Availability of data and materials. VCF files used to complete computational analyses are available by reasonable request, code is publicly available on Github (refer to Methods), physical materials used are referred to by their product codes.

Competing interest.

All authors declare no competing interests.

Funding. This study was supported by the Canadian Institutes for Health Research (CIHR 476575) to JDSW, and an operating grant to the Coronavirus Variants Rapid Response Network (CoVaRR-Net) to LF and IR and CIHR grant (GA1-117694) to LF. The funding body had no role in the design of the study or collection, analysis, interpretation, or reporting of the data.

Authors contributions. Julian Daniel Sunday Willett conceived of the computational analyses needed for this study, completed all computational analysis of viral sequencing data, and wrote the majority of the manuscript. Louis Flamand and Jiannis Ragoussis conceived of the study. Louis Flamand contributed to manuscript revisions, wrote sections relevant to animal models and antibody neutralization studies and performed analysis of results. Jiannis Ragoussis supervised sequencing data generation and analysis. Isabelle Dubuc and Leslie Gudimard performed all works involving live SARS-CoV-2 viruses. Annie Gravel participated in the sequence analysis and methodological design of experiments. Paul Fortin and Ines Colmegna provided key reagents. Jose Hector Galvez contributed bioinformatics analysis review and

402 manuscript revisions. Ju-Ling Liu, Anne-Marie Roy, Sally Lee and Shu-Huang Chen supported
403 the SARS-CoV-2 viral sequencing.

404 ***Acknowledgments***.

405 This research was enabled in part by support provided by Calcul Québec (calculquebec.ca) and
406 the Digital Research Alliance of Canada (alliancecan.ca). This work was made possible by
407 funding from the CIHR as part of CoVaRR-Net (to JR and LF) . We thank Ines Colmegna for
408 providing vaccinated patient sera. We thank Silvia Vidal for her guidance regarding SARS-CoV-
409 2 evolutionary mechanisms.

410

411 **References**:

412 1. Jacobs JL, Haidar G, Mellors JW. COVID-19: Challenges of Viral Variants. Annu Rev
413 Med. 2022.
414 2. Sun F, Wang X, Tan S, Dan Y, Lu Y, Zhang J, et al. SARS-CoV-2 Quasispecies
415 Provides an Advantage Mutation Pool for the Epidemic Variants. Microbiol Spectr.
416 2021;9(1):e0026121.
417 3. Velavan TP, Pallerla SR, Ruter J, Augustin Y, Kremsner PG, Krishna S, et al. Host
418 genetic factors determining COVID-19 susceptibility and severity. EBioMedicine.
419 2021;72:103629.
420 4. Belsky JA, Tullius BP, Lamb MG, Sayegh R, Stanek JR, Auletta JJ. COVID-19 in
421 immunocompromised patients: A systematic review of cancer, hematopoietic cell and solid
422 organ transplant patients. J Infect. 2021;82(3):329-38.
423 5. Van Cleemput J, van Snippenberg W, Lambrechts L, Dendooven A, D'Onofrio V, Couck
424 L, et al. Organ-specific genome diversity of replication-competent SARS-CoV-2. Nat Commun.
425 2021;12(1):6612.

426 6. Wang R, Chen J, Wei GW. Mechanisms of SARS-CoV-2 Evolution Revealing Vaccine-
427 Resistant Mutations in Europe and America. J Phys Chem Lett. 2021;12(49):11850-7.
428 7. Liu Y, Liu J, Plante KS, Plante JA, Xie X, Zhang X, et al. The N501Y spike substitution
429 enhances SARS-CoV-2 infection and transmission. Nature. 2022;602(7896):294-9.
430 8. Motozono C, Toyoda M, Zahradnik J, Saito A, Nasser H, Tan TS, et al. SARS-CoV-2
431 spike L452R variant evades cellular immunity and increases infectivity. Cell Host Microbe.
432 2021;29(7):1124-36 e11.
433 9. Cherian S, Potdar V, Jadhav S, Yadav P, Gupta N, Das M, et al. SARS-CoV-2 Spike
434 Mutations, L452R, T478K, E484Q and P681R, in the Second Wave of COVID-19 in
435 Maharashtra, India. Microorganisms. 2021;9(7).
436 10. Liu Y, Liu J, Johnson BA, Xia H, Ku Z, Schindewolf C, et al. Delta spike P681R mutation
437 enhances SARS-CoV-2 fitness over Alpha variant. Cell Rep. 2022;39(7):110829.
438 11. Planas D, Veyer D, Baidaliuk A, Staropoli I, Guivel-Benhassine F, Rajah MM, et al.
439 Reduced sensitivity of SARS-CoV-2 variant Delta to antibody neutralization. Nature.
440 2021;596(7871):276-80.
441 12. Gu H, Chen Q, Yang G, He L, Fan H, Deng YQ, et al. Adaptation of SARS-CoV-2 in
442 BALB/c mice for testing vaccine efficacy. Science. 2020;369(6511):1603-7.
443 13. Wasik BR, Voorhees IEH, Barnard KN, Alford-Lawrence BK, Weichert WS, Hood G, et
444 al. Influenza Viruses in Mice: Deep Sequencing Analysis of Serial Passage and Effects of Sialic
445 Acid Structural Variation. J Virol. 2019;93(23).
446 14. Sun S, Gu H, Cao L, Chen Q, Ye Q, Yang G, et al. Characterization and structural basis
447 of a lethal mouse-adapted SARS-CoV-2. Nat Commun. 2021;12(1):5654.
448 15. Huang K, Zhang Y, Hui X, Zhao Y, Gong W, Wang T, et al. Q493K and Q498H
449 substitutions in Spike promote adaptation of SARS-CoV-2 in mice. EBioMedicine.
450 2021;67:103381.

451 16. Chung H, Noh JY, Koo BS, Hong JJ, Kim HK. SARS-CoV-2 mutations acquired during
452 serial passage in human cell lines are consistent with several of those found in recent natural
453 SARS-CoV-2 variants. Comput Struct Biotechnol J. 2022;20:1925-34.
454 17. Sonnleitner ST, Sonnleitner S, Hinterbichler E, Halbfurter H, Kopecky DBC, Koblmuller
455 S, et al. The mutational dynamics of the SARS-CoV-2 virus in serial passages in vitro. Virol Sin.
456 2022;37(2):198-207.
457 18. Lei C, Yang J, Hu J, Sun X. On the Calculation of TCID(50) for Quantitation of Virus
458 Infectivity. Virol Sin. 2021;36(1):141-4.
459 19. Garrison EPMG. Haplotype-based variant detection from short-read sequencing. arXiv.
460 2012.
461 20. Tonkin-Hill G, Martincorena I, Amato R, Lawson AR, Gerstung M, Johnston I, et al.
462 Patterns of within-host genetic diversity in SARS-CoV-2. Elife. 2021;10.
463 21. N'Guessan A TA, Sanchez-Quete F, Goitom E, Reiling SJ, Galvez JH, Nguyen TL,
464 Nguyen HTL, Visentin F, Hachad M, Krylova K, Matthews S, Kraemer SA, Stretenowich P,
465 Bourgey M, Djambazian H, Chen S, Roy A, Brookes B, Lee S, Simon M, Maere T,
466 Vanrolleghem PA, Labelle M, Moreira S, Levade I, Bourque G, Ragoussis J, Dorner S, Frigon
467 D, Shapiro BJ. Detection of prevalent SARS-CoV-2 variant lineages in wastewater and clinical
468 sequences from cities in Québec, Canada. medRxiv. 2022.
469 22. Gerstung M, Beisel C, Rechsteiner M, Wild P, Schraml P, Moch H, et al. Reliable
470 detection of subclonal single-nucleotide variants in tumour cell populations. Nat Commun.
471 2012;3:811.
472 23. Rao RSP, Ahsan N, Xu C, Su L, Verburgt J, Fornelli L, et al. Evolutionary Dynamics of
473 Indels in SARS-CoV-2 Spike Glycoprotein. Evol Bioinform Online.
474 2021;17:11769343211064616.
475 24. Ramachandran VK, Khalifa MS, Lilley CJ, Brown MR, van Aerle R, Denise H, et al.
476 Comparison of variant callers for wastewater-based epidemiology. medRxiv. 2022.

477 25. Li H. Aligning sequence reads, clone sequences and assembly contigs with BWA-MEM.
478 arXiv. 2013.
479 26. McLaren W, Gil L, Hunt SE, Riat HS, Ritchie GR, Thormann A, et al. The Ensembl
480 Variant Effect Predictor. Genome Biol. 2016;17(1):122.
481 27. Kent WJ, Sugnet CW, Furey TS, Roskin KM, Pringle TH, Zahler AM, et al. The human
482 genome browser at UCSC. Genome Res. 2002;12(6):996-1006.
483 28. Turakhia Y, Thornlow B, Hinrichs A, McBroome J, Ayala N, Ye C, et al. Pandemic-scale
484 phylogenomics reveals the SARS-CoV-2 recombination landscape. Nature.
485 2022;609(7929):994-7.
486 29. Cao Y, Yisimayi A, Jian F, Song W, Xiao T, Wang L, et al. BA.2.12.1, BA.4 and BA.5
487 escape antibodies elicited by Omicron infection. Nature. 2022;608(7923):593-602.
488 30. Johnson BA, Xie X, Bailey AL, Kalveram B, Lokugamage KG, Muruato A, et al. Loss of
489 furin cleavage site attenuates SARS-CoV-2 pathogenesis. Nature. 2021;591(7849):293-9.
490 31. Tada T, Dcosta BM, Samanovic MI, Herati RS, Cornelius A, Zhou H, et al.
491 Convalescent-Phase Sera and Vaccine-Elicited Antibodies Largely Maintain Neutralizing Titer
492 against Global SARS-CoV-2 Variant Spikes. mBio. 2021;12(3):e0069621.
493 32. Dupont L, Snell LB, Graham C, Seow J, Merrick B, Lechmere T, et al. Neutralizing
494 antibody activity in convalescent sera from infection in humans with SARS-CoV-2 and variants
495 of concern. Nat Microbiol. 2021;6(11):1433-42.
496 33. Tarres-Freixas F, Trinite B, Pons-Grifols A, Romero-Durana M, Riveira-Munoz E, Avila-
497 Nieto C, et al. Heterogeneous Infectivity and Pathogenesis of SARS-CoV-2 Variants Beta, Delta
498 and Omicron in Transgenic K18-hACE2 and Wildtype Mice. Front Microbiol. 2022;13:840757.
499 34. Rahimi F, Talebi Bezmin Abadi A. Implications of the Emergence of a New Variant of
500 SARS-CoV-2, VUI-202012/01. Arch Med Res. 2021;52(5):569-71.
501 35. Sedova M, Jaroszewski L, Iyer M, Godzik A. Monitoring for SARS-CoV-2 drug resistance
502 mutations in broad viral populations. bioRxiv. 2022.

503 36. Kandeel M, Abdelrahman AHM, Oh-Hashi K, Ibrahim A, Venugopala KN, Morsy MA, et
504 al. Repurposing of FDA-approved antivirals, antibiotics, anthelmintics, antioxidants, and cell
505 protectives against SARS-CoV-2 papain-like protease. J Biomol Struct Dyn. 2021;39(14):5129-
506 36.
507 37. Hammond J, Leister-Tebbe H, Gardner A, Abreu P, Bao W, Wisemandle W, et al. Oral
508 Nirmatrelvir for High-Risk, Nonhospitalized Adults with Covid-19. N Engl J Med.
509 2022;386(15):1397-408.
510 38. Pastorio C, Zech F, Noettger S, Jung C, Jacob T, Sanderson T, et al. Determinants of
511 Spike infectivity, processing, and neutralization in SARS-CoV-2 Omicron subvariants BA.1 and
512 BA.2. Cell Host Microbe. 2022;30(9):1255-68 e5.
513 39. Zeng C, Evans JP, Faraone JN, Qu P, Zheng YM, Saif L, et al. Neutralization of SARS-
514 CoV-2 Variants of Concern Harboring Q677H. mBio. 2021;12(5):e0251021.
515 40. Kim K, Calabrese P, Wang S, Qin C, Rao Y, Feng P, et al. The roles of APOBEC-
516 mediated RNA editing in SARS-CoV-2 mutations, replication and fitness. Sci Rep.
517 2022;12(1):14972.

518

Figures:

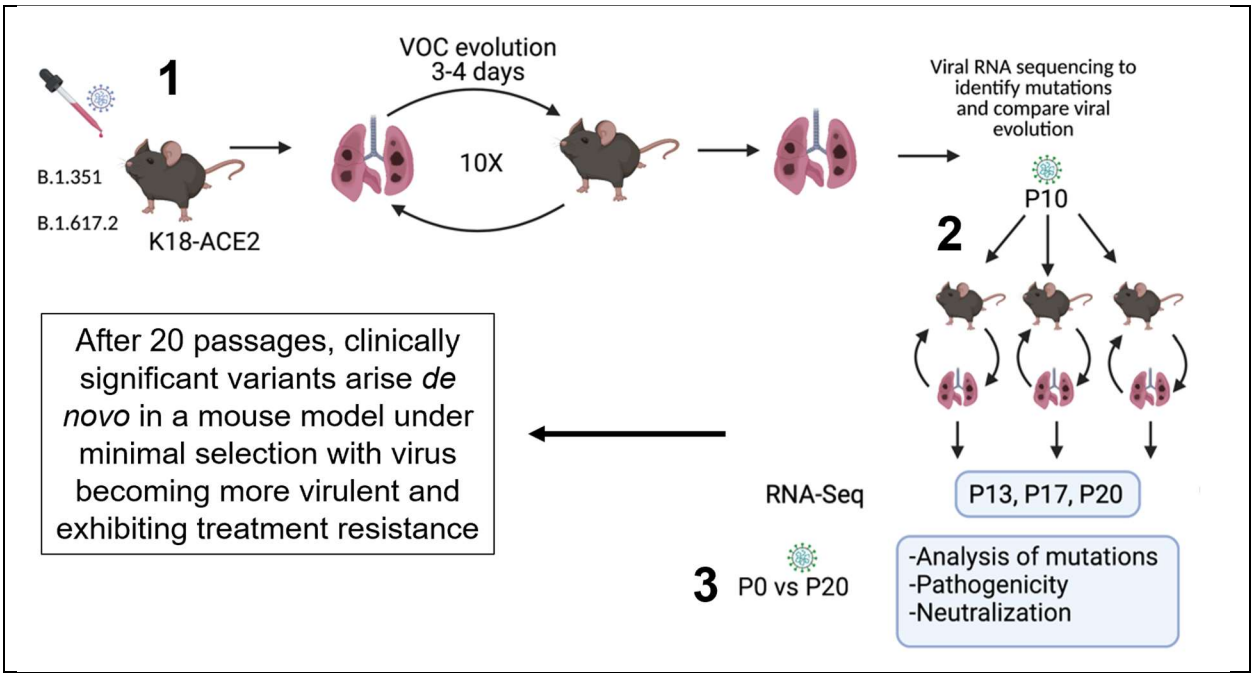

Figure 1.

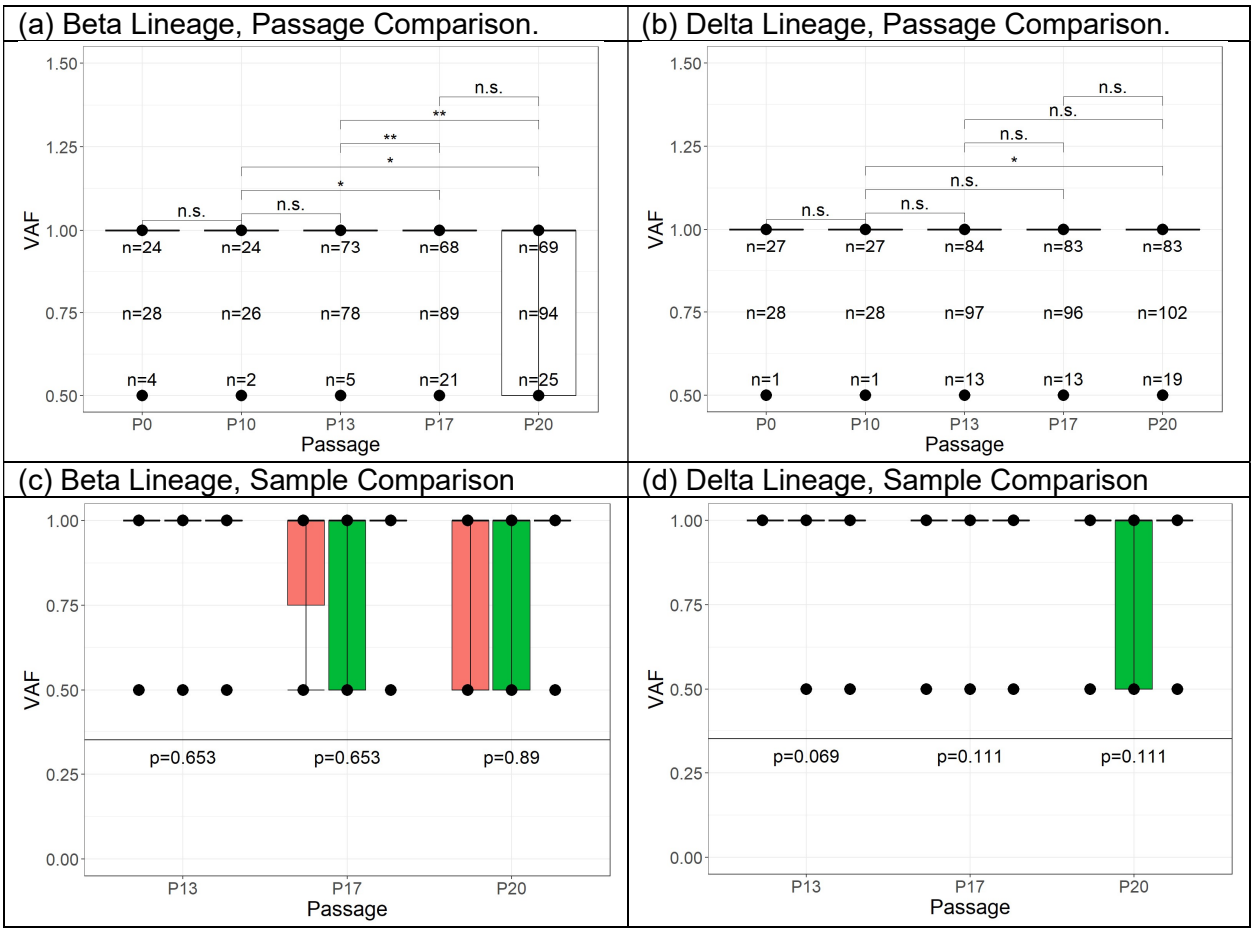
(a) Beta Lineage, Passage Comparison.
(b) Delta Lineage, Passage Comparison.
(c) Beta Lineage, Sample Comparison
(d) Delta Lineage, Sample Comparison
VAF
Passage
P0
P10
P13
P17
P20
n.s.
*
**
n=24
n=24
n=73
n=68
n=69
n=28
n=26
n=78
n=89
n=94
n=4
n=2
n=5
n=21
n=25
n=27
n=27
n=84
n=83
n=83
n=28
n=28
n=97
n=96
n=102
n=1
n=1
n=13
n=13
n=19
p=0.653
p=0.653
p=0.89
p=0.069
p=0.111
p=0.111

Figure 2.

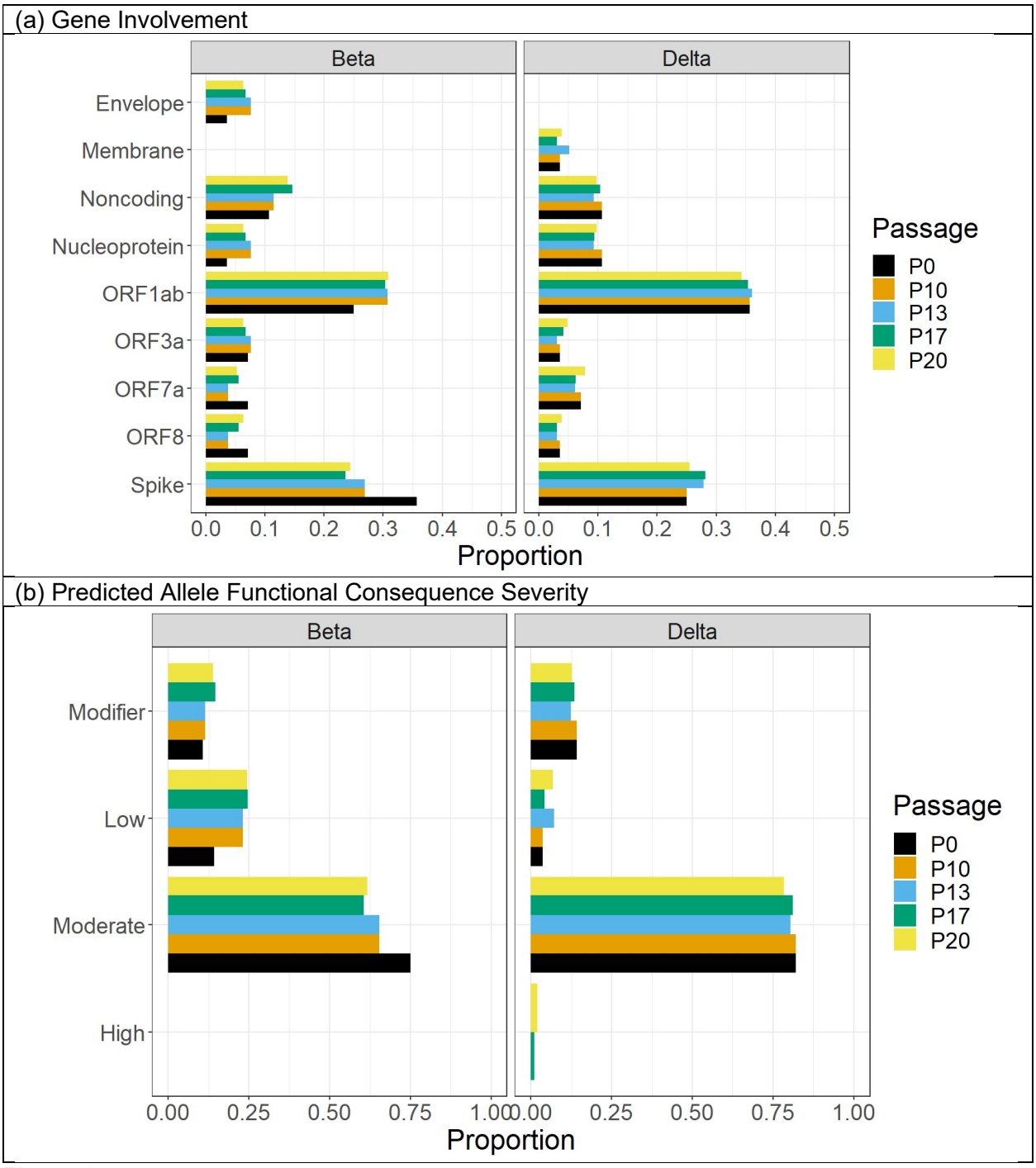
(a) Gene Involvement
Beta
Delta
Envelope
Membrane
Noncoding
Nucleoprotein
ORF1ab
ORF3a
ORF7a
ORF8
Spike
0.0
0.1
0.2
0.3
0.4
0.5
Proportion
Passage
P0
P10
P13
P17
P20
(b) Predicted Allele Functional Consequence Severity
Beta
Delta
Modifier
Low
Moderate
High
0.00
0.25
0.50
0.75
1.00
Proportion
Passage
P0
P10
P13
P17
P20

Figure 3.

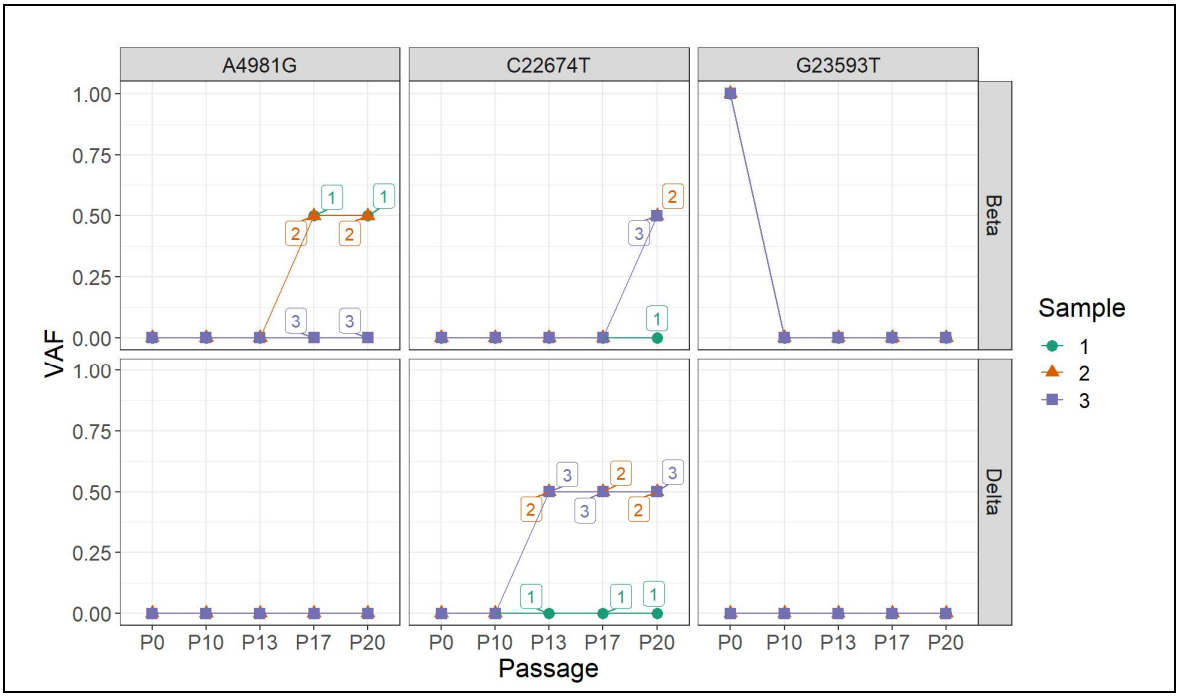
A4981G
C22674T
G23593T
Beta
Delta
VAF
1.00
0.75
0.50
0.25
0.00
P0
P10
P13
P17
P20
Passage
Sample
1
2
3

Figure 4.

Table 1.

Variant	Amino Acid Change	Annotation
A4981G	ORF1ab T1572T	Mutations that may confer drug resistance[1]
C22674T	Spike S371F	Protein interacting, antibody escape, vaccine target, Omicron-associated variant allele[1]
G23593T	Spike Q677H	Protein interacting, vaccine target[1], enhances treatment resistance[2], increases infectivity[2]

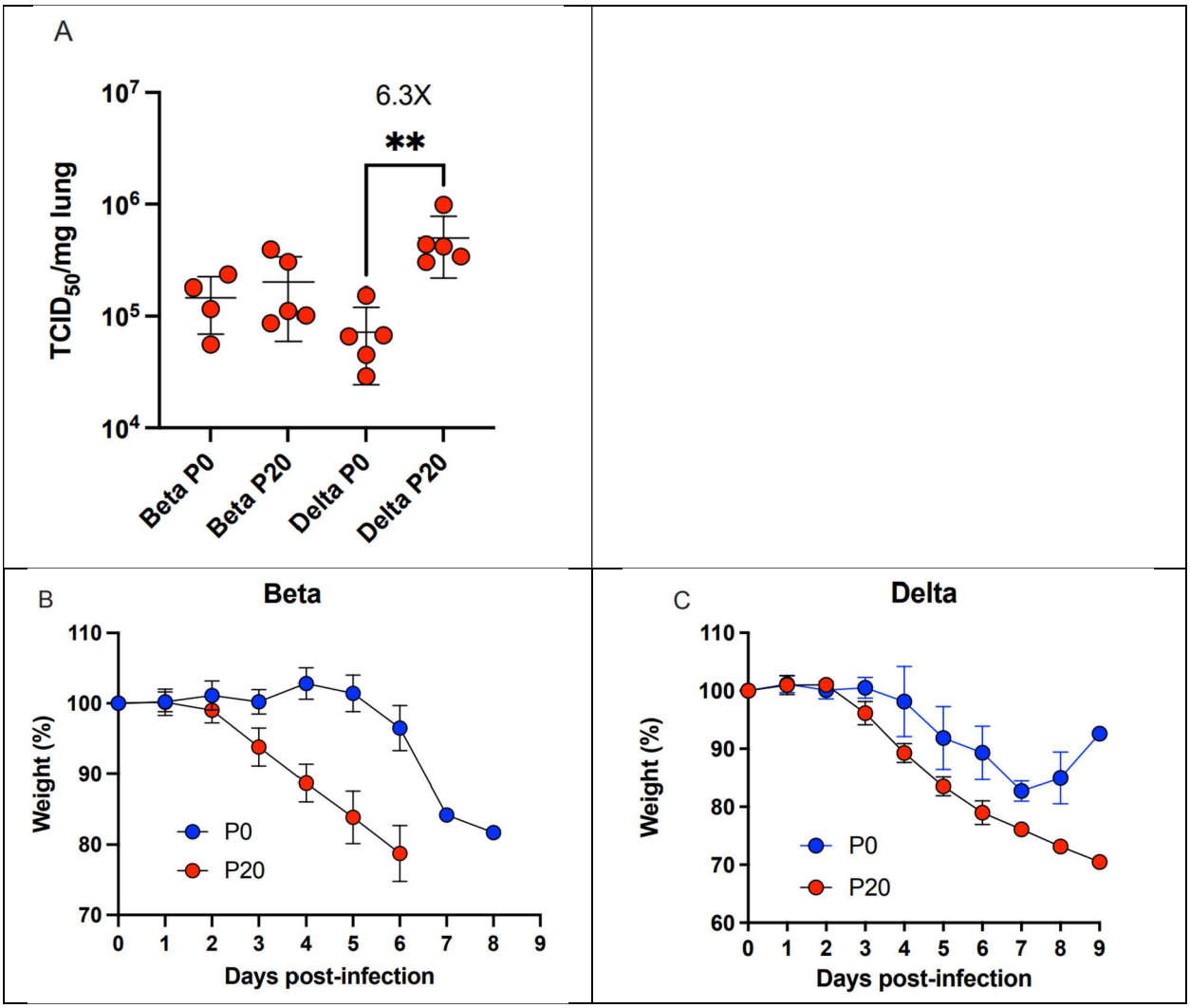
A
6.3X
**
TCID50/mg lung
10^7
10^6
10^5
10^4
Beta P0
Beta P20
Delta P0
Delta P20
B
Beta
Weight (%)
110
100
90
80
70
P0
P20
0 1 2 3 4 5 6 7 8 9
Days post-infection
C
Delta
Weight (%)
110
100
90
80
70
60
P0
P20
0 1 2 3 4 5 6 7 8 9
Days post-infection

Figure 5.

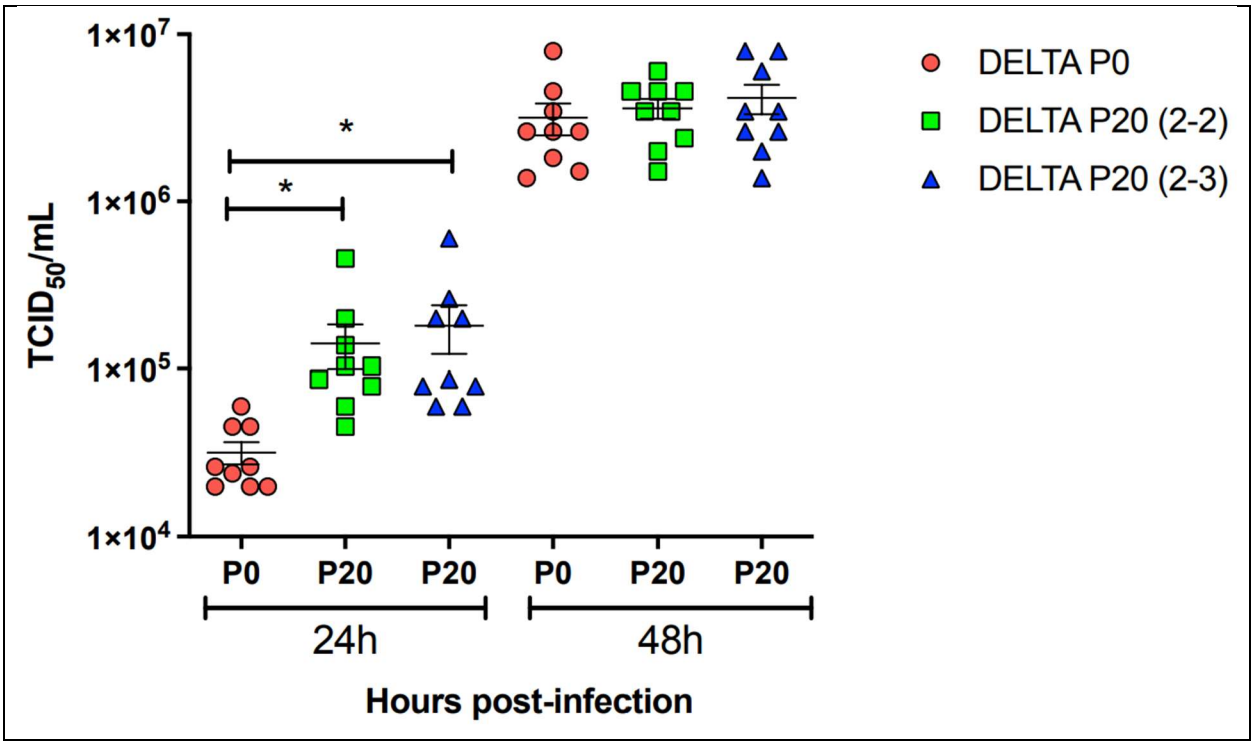
1×10^7
1×10^6
1×10^5
1×10^4
TCID50/mL
*
*
P0
P20
P20
P0
P20
P20
24h
48h
Hours post-infection
DELTA P0
DELTA P20 (2-2)
DELTA P20 (2-3)

Figure 6.

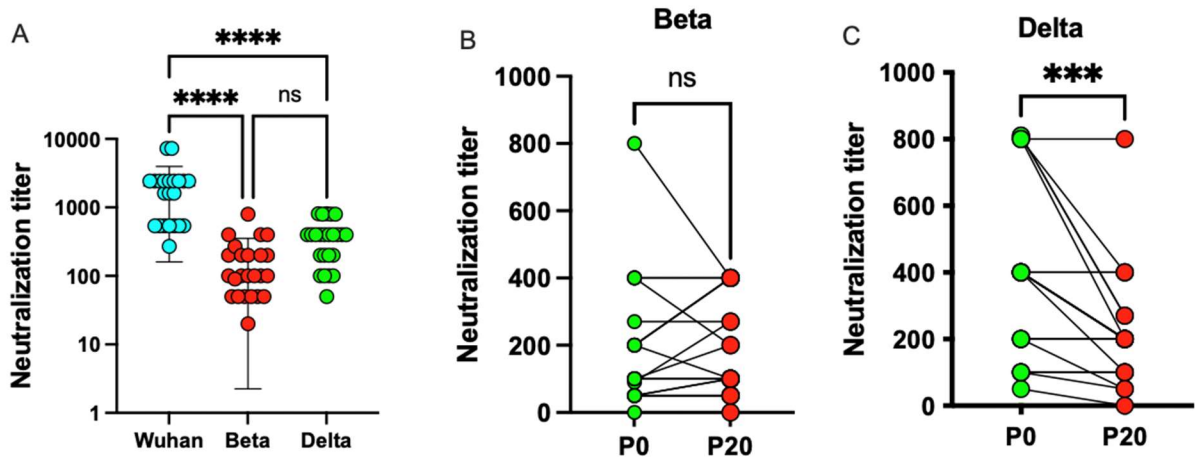
A
****
****
ns
Neutralization titer
10000
1000
100
10
1
Wuhan
Beta
Delta
B
Beta
ns
Neutralization titer
1000
800
600
400
200
0
P0
P20
C
Delta
***
Neutralization titer
1000
800
600
400
200
0
P0
P20

Figure 7.

Supplemental Figures

Supplemental Table 1.

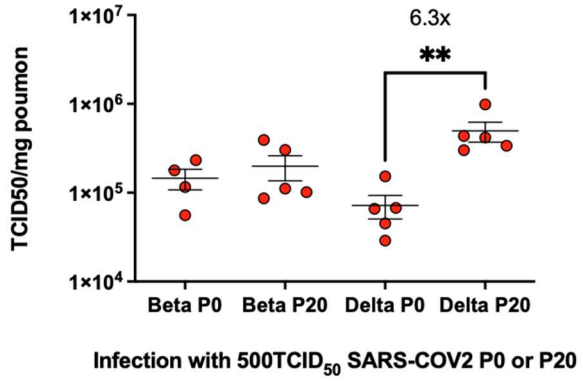

Supplemental Figure 1.

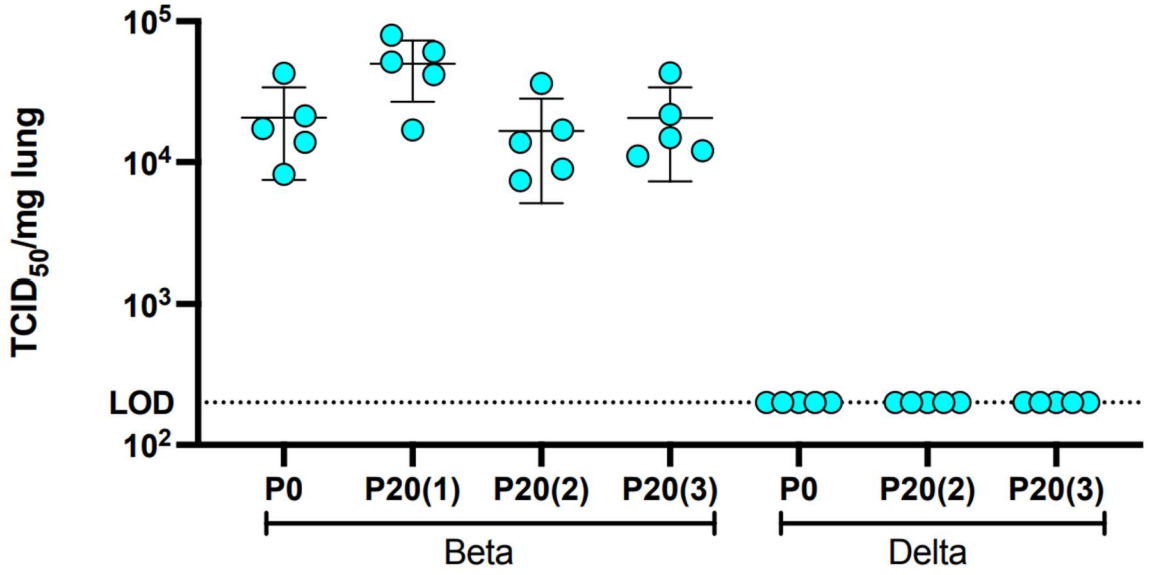

Supplementary Figure 2.

Figure References.

1. Kent, W.J., Sugnet, C.W., Furey, T.S., Roskin, K.M., Pringle, T.H., Zahler, A.M., and Haussler, D. (2002). The human genome browser at UCSC. Genome Res *12*, 996-1006. 10.1101/gr.229102.
2. Zeng, C., Evans, J.P., Faraone, J.N., Qu, P., Zheng, Y.M., Saif, L., Oltz, E.M., Lozanski, G., Gumina, R.J., and Liu, S.L. (2021). Neutralization of SARS-CoV-2 Variants of Concern Harboring Q677H. mBio *12*, e0251021. 10.1128/mBio.02510-21.